

ORIGINAL ARTICLE

Three-dimensional evaluation of thoracic aorta enlargement and unfolding in hypertensive men using non-contrast computed tomography

D Craiem^{1,2}, G Chironi^{1,3,4}, ME Casciaro², A Redheuil^{3,5,6}, E Mousseaux^{3,5,6} and A Simon^{1,3,4}

Aging produces a simultaneous thoracic aorta (TA) enlargement and unfolding. We sought to analyze the impact of hypertension on these geometric changes. Non-contrast computed tomography images were obtained from coronary artery calcium scans, including the entire aortic arch, in 200 normotensive and 200 hypertensive asymptomatic men. An automated algorithm reconstructed the vessel in three-dimensions, estimating orthogonal aortic sections along the whole TA pathway, and calculated several geometric descriptors to assess TA morphology. Hypertensive patients were older with respect to normotensive ($P < 0.001$). Diameter and volume of TA ascending, arch and descending segments were higher in hypertensive patients with respect to normotensive ($P < 0.001$) and differences persisted after adjustment for age. Hypertension produced an accelerated unfolding effect on TA shape. We found increments in aortic arch width ($P < 0.001$), radius of curvature ($P < 0.001$) and area under the arch curve ($P < 0.01$) with a concomitant tortuosity decrease ($P < 0.05$) and no significant change in aortic arch height. Overall, hypertension produced an equivalent effect of 2–7-years of aging. In multivariate analysis adjusted for age and hypertension treatment, diastolic pressure was more associated to TA size and shape changes than systolic pressure. These data suggest that hypertension accelerates TA enlargement and unfolding deformation with respect to the aging effect.

Journal of Human Hypertension advance online publication, 24 January 2013; doi:10.1038/jhh.2012.69

Keywords: thoracic aorta 3D reconstruction; non-contrast MSCT; aortic arch uncoiling; aging; tridimensional image segmentation

INTRODUCTION

The thoracic aorta (TA) is subject to progressive size increase and a concomitant unfolding process.^{1–3} The noninvasive assessment of TA geometry was employed to better predict aneurisms, preventing complications as dissection or rupture⁴ and also to provide basic information for development of endovascular devices for the aortic arch.^{5,6} TA size assessment is traditionally based on the measurement of aortic diameter.^{3,7} However, diameter estimation may be a source of error^{3,7,8} because TA shape is complex with a curvilinear pathway that produces oblong contours using axial planes.⁴ Also, TA size is not reflected solely by diameter because the TA length is another determinant of the vessel size.^{4,9,10} Taking into account these considerations, we have recently validated a new automated tool, based on the computerized reconstruction and analysis of orthogonal sections and lengths of ascending, arch and descending TA segments.¹¹ Briefly, this tool allows for a virtual three-dimensional reconstruction and assessment of the vessel size and shape. This methodology was specifically designed to evaluate patients referred to our department for non-contrast multislice computed tomography assessment of coronary artery calcium (CAC) in view of cardiovascular risk refinement.^{8,12,13} Measurements can be done on routine scans, extending the field of view to cover the top of the aortic arch.

Hypertension was identified as a major determinant of aortic size^{8,14,15} but its simultaneous influence on the aortic size and

shape was less investigated. The aim of the present study was to assess the impact of hypertension on TA geometry, expressed in terms of an equivalent aging factor. Several descriptors were proposed to accurately describe the deformation of the TA curvilinear portion, focusing on its three-dimensional shape.

SUBJECTS AND METHODS

Study subjects

Individuals were initially screened by occupational health physicians or general internists. Those with the presence of at least one established risk factor for coronary heart disease, such as advanced age, hypertension, hypercholesterolemia, diabetes mellitus or current smoking, were referred to hospital for atherosclerosis imaging-based risk management. In the present study, we included 200 normotensive and 200 hypertensive men that fulfilled the two following criteria: they had no symptom of known history of cardiovascular disease, including coronary heart disease, stroke and peripheral vascular disease; and they had undergone noncontrast cardiac computed tomography (CT) for CAC screening during their hospitalization between September 2009 and October 2010. The retrospective analysis of personal health data of study subjects had the authorization of the *Commission nationale de l'informatique et des libertés* and was in accordance with the declaration of Helsinki.

Risk factors

All risk factors were measured at the same time as aortic imaging. Weight and height were measured for calculation of body surface area. Brachial

¹Centre de Médecine Préventive Cardiovasculaire, Hôpital Européen Georges Pompidou, APHP, Paris, France; ²Universidad Favaloro, CONICET, Buenos Aires, Argentina; ³Université Paris Descartes, Sorbonne Paris Cité, Faculté de Médecine, Paris, France; ⁴Centre de Recherche Cardiovasculaire de l'HEGP (INSERM U970), Paris, France; ⁵Département de Radiologie Cardiovasculaire, Hôpital Européen Georges Pompidou, APHP, Paris, France and ⁶Unité INSERM 678, Paris, France. Correspondence: Dr D Craiem, Universidad Favaloro (FICEN), Av. Belgrano 1723, C.P. 1093, Buenos Aires, Argentina.

E-mail: dcraiem@favaloro.edu.ar

Received 29 August 2012; revised 11 December 2012; accepted 17 December 2012

blood pressure (BP) was determined as the mean of three measurements by sphygmomanometer procedure in the supine position after 10 min rest. Hypertension was defined by BP of 140 or 90 mm Hg or above, or presence of hypertensive medication. Total and high-density lipoprotein blood cholesterol and triglyceride were measured in the supine position after 14-h fasting and low-density lipoprotein was calculated with the Friedewald formula or, if not applicable, directly measured. Hypercholesterolemia was defined by fasting low-density lipoprotein cholesterol above 3.3 mmol l^{-1} or by presence of low-density lipoprotein-lowering drug treatment. Blood glucose was measured after overnight fast and diabetes was defined by fasting blood glucose of 7 mmol l^{-1} or above, or by presence of antidiabetic medication. Past or current smokers were defined as subjects who smoke or had smoked at least on cigarette per day, every day or some day. Clinical characteristics are shown in Table 1. Comparing hypertensive with respect to normotensive subjects, only age and BP were significantly higher, whereas body surface area and the proportion of patients that had hypercholesterolemia ($\approx 80\%$), diabetes ($\approx 10\%$) or smokers ($\approx 60\%$) resulted similar.

Image acquisition

Aortic imaging was obtained with non-contrast cardiac 64-slice multislice computed tomography (Light-speed VCT; GE Health care, Milwaukee, WI, USA) during the acquisition done to quantify CAC. Measures were done with 2.5-mm axial slices, 120 kVp, 250-mA tube current, 250-ms exposure time and a 250-mm field of view. Images were acquired with prospective-electrocardiography gating at 60% of R-R interval in the cranio-caudal direction from the top of the aortic arch to the level of the diaphragm. Scans were exported as DICOM files and analyzed by a custom-designed software that estimated the three-dimensional TA geometry.¹¹

Aortic size and shape measurements

Details of the automated tool can be found elsewhere.¹¹ In a first step, the technician identifies the CT axial slice corresponding to the level of the pulmonary artery bifurcation, in which sections of ascending and descending aorta are approximately circular (Figure 1). Then, two seed points inside the aortic cross-sections are manually set and an automated process begins. First, a circle fitting algorithm finds the largest circle inscribed into the cross-sectional area. The centers of the circles, C_A and C_D , are adopted as aortic centerline points (Figure 1). In a second step, the rectilinear portion of the TA (downstream to C_D) is analyzed, applying the circle fitting algorithm to the aortic sections to estimate centerline points of the descending aorta (Figure 2a). In a third step, the curvilinear portion of the TA (upstream to C_A) is measured reconstructing oblique planes that follow the aortic curvature. The planes were calculated using a trilinear interpolation and pivoting by incremental two-degree angle around the arch center (midpoint between C_A and C_D) as shown in Figure 2b. Aortic sections in the corresponding planes are approximately circular and then centerline points are accurately assessed. The distance between two centerline points in the curvilinear portion was determined by the two-degree angle step, that is, $2.8 \pm 0.3 \text{ mm}$ (Figure 2b). Once all centerline points were obtained for the whole TA (black points in Figure 2b), the aortic centerline is automatically reconstructed with a cubic spline. For each centerline point, orthogonal planes to the centerline curve are calculated (Figure 2c) and definitive aortic circular sections are estimated with the circle fitting algorithm, assigning a diameter value to each

centerline point and allowing the reconstruction of the aortic volume in a three-dimensional space.^{11,16}

The vessel was divided into three anatomical segments by appropriate orthogonal planes (Figure 2c): (i) the ascending aorta, beginning at the plane corresponding to the left main coronary artery and extending to the plane corresponding to the origin of the brachiocephalic artery; (ii) the aortic arch, beginning at the brachiocephalic artery plane and extending to the plane corresponding to the origin of the left subclavian artery; (iii) the descending aorta beginning at the left subclavian artery plane and extending to the coronary sinus. In each TA segment, diameter, volume and length are automatically measured.

For the curvilinear portion that goes from C_A at 0° to C_D at 180° , several shape descriptors were assessed as shown in Figure 3: the aortic arch width and height, the radius of curvature defined in,¹⁷ the aortic tortuosity calculated as one minus the ratio of curve length to the straight line distance between endpoints,¹¹ the aortic tapering defined as the difference between descending and ascending diameters over the curvilinear length, the distance from arch center to C_{45° and C_{135° coordinates and the area under the curve (AUC).

Duplicate readings of the same scans showed maximum coefficient of variation values of 0.3% for TA diameter and 4% for TA volume. Maximum interobserver variability was 0.4% and 4.4% for TA diameter and volume, respectively.¹¹

Statistical analysis

Baseline characteristics of normotensive and hypertensive subjects were compared by use of a χ^2 statistic for dichotomous variables and analysis of variance for continuous variables. Size and shape measurements were informed as mean \pm s.d. for each group and were analyzed in terms of hypertension presence in a multivariate model adjusted for age. The parameter estimates of the linear regression analysis indicate the change per 10 years age ($\beta_{\text{AGE}} \pm \text{s.e.}$) and the presence (vs absence) of hypertension ($\beta_{\text{HTA}} \pm \text{s.e.}$). The quotient $\beta_{\text{HTA}} \times 10 / \beta_{\text{AGE}}$ was proposed to quantify an equivalent of aging (in years) for the presence of hypertension. The percentage change of geometrical measurements was calculated with respect to normotensive values, adopted as a reference. Additional multivariate models, adjusted for age and hypertension treatment, were calculated by entering geometrical measurements as dependent variables and diastolic or systolic BP as independent variables. Statistical analysis was performed with JMP (SAS NC USA) software and significance was set at $P < 0.05$.

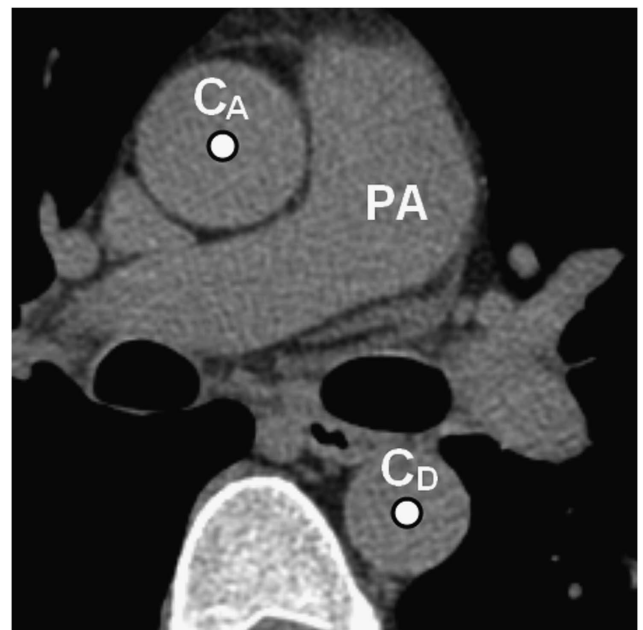


Figure 1. Initial seed points for the automated algorithm. Circular sections of ascending and descending aorta in the CT slice at the pulmonary artery (PA) bifurcation level. C_A and C_D show the ascending and descending aorta centers.

Table 1. Clinical characteristics of the study population

	Normotensive	Hypertensive	P
Number of men	200	200	—
Age, years	54 ± 8	59 ± 8	< 0.001
Body surface area, m^2	1.98 ± 0.14	2.00 ± 0.15	NS
Hypertension treatment, n(%)	0	179 (90)	—
Blood pressure, mm Hg			
Systolic	120 ± 9	128 ± 14	< 0.001
Diastolic	73 ± 7	76 ± 10	< 0.001
Pulse	47 ± 7	52 ± 9	< 0.001
Hypercholesterolemia, n (%)	154 (80)	169 (84)	NS
Diabetes, n (%)	13 (7)	26 (13)	< 0.05
Past or current smoking, n (%)	125 (64)	108 (56)	NS

Abbreviation: NS, non significant. Data are mean \pm s.d. or number of patients n (%).

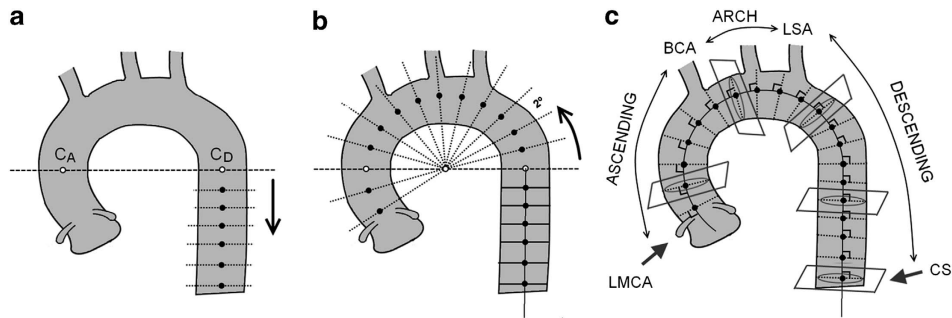


Figure 2. Schematic representation of the process to measure TA dimensions. (a), rectilinear descending aorta centerline points downstream C_D (see Figure 1) in CT axial slices spaced out 2.5 mm apart. (b), curvilinear aorta portion centerline points upstream C_D in orthogonal planes pivoting by 2° angle increment around the midpoint between C_D and C_A (see Figure 1) and spaced out 2.8 ± 0.3 mm apart. (c), aortic circular sections in planes orthogonal to total TA centerline. BCA: brachiocephalic artery; CS: coronary sinus; LMCA: left main coronary artery; LSA: left subclavian artery. C_A and C_D design centers of ascending and descending TA.

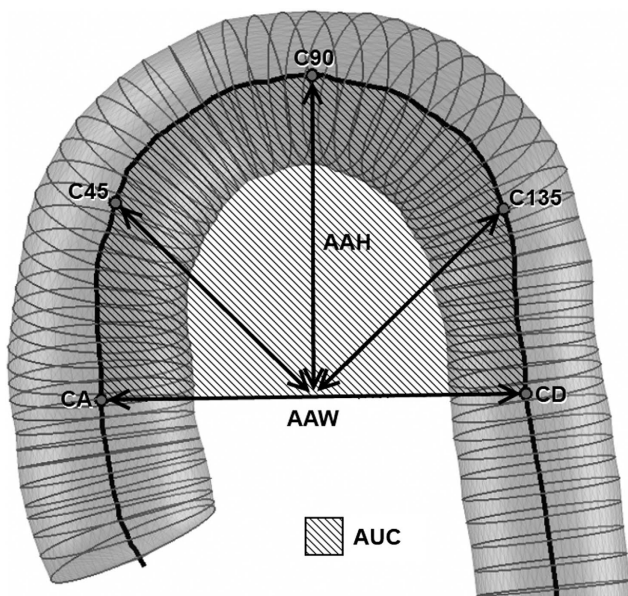


Figure 3. Morphologic descriptors for the TA curvilinear portion. AAW: aortic arch width; AAH: aortic arch height; AUC: area under the curve; C_A and C_D design centers of ascending and descending TA.

RESULTS

Table 2 shows absolute geometric values for normotensive and hypertensive patients. In hypertensive subjects, ascending, arch and descending TA segments were larger with respect to normotensive ($P < 0.001$). Diameters were 5–7% and volumes 16–22% higher ($P < 0.001$). In the aortic curvilinear portion (semi-arc from 0° – 180°), an unfolding effect was evidenced with hypertension. The arch was 9% wider ($P < 0.001$), the radius of curvature increased 8% ($P < 0.001$), tortuosity decreased 6% ($P < 0.01$) and the AUC grew 14% ($P < 0.001$). The vectors from the arch center to the posterior (C_{135°) and anterior (C_{45°) sections increased 8% and 6%, respectively ($P < 0.001$). Aortic tapering was more pronounced during hypertension (+6%) although it did not attain significance ($P = 0.06$). When variables were adjusted for age, all changes remained significant between normotensive and hypertensive subjects ($P < 0.001$ for diameters, volumes arch width, radius of curvature and distance from center to C_{135° , $P < 0.01$ for the curvilinear length, distance from center to C_{45° and AUC, $P < 0.05$ for tortuosity) except for aortic arch height and

tapering (Table 2, right). The presence of hypertension resulted equivalent to an aging of 5-years in ascending, 5–6-years in arch and 2–4-years in descending TA segments. In the curvilinear portion, the presence of hypertension was equivalent to an aging of 8-years for radius of curvature, 7-years for tortuosity and 4-years for the arch width. The equivalence for distance from arch center to C_{135° and AUC was 3-years of aging.

Table 3 shows the associations of TA size and shape measures with systolic and diastolic BP after adjusting for age and current drug treatments. Diastolic BP was positively associated with TA size ($P < 0.001$ for diameters and volumes for the 3 segments). Also, a positive association was found with the arch width ($P < 0.001$), radius of curvature ($P < 0.01$), arch center to C_{45° and C_{135° distances ($P < 0.001$) and AUC ($P < 0.001$). Systolic BP was positively associated with TA size in the arch ($P < 0.01$) and the descending segment ($P < 0.001$) but only marginally with the ascending portion ($P < 0.05$ for diameter). Also, a positive association was found between systolic BP and the arch width ($P < 0.001$), radius of curvature ($P < 0.01$) and arch center to C_{135° distance ($P < 0.05$) whereas a negative relation was found with tortuosity ($P < 0.05$). The most sensitive variable was the arch width, that widened 12% with a 10 mm Hg increase in systolic BP ($P < 0.001$). The aortic arch height and tapering were not associated to BP components.

DISCUSSION

This study provides an exhaustive description of the TA geometry assessed non-invasively by non-contrast multislice computed tomography in asymptomatic adults in relation with hypertension. The main result is that the presence of hypertension accelerates the TA enlargement in its three portions and significantly widens the aortic arch. If the TA size is evaluated in terms of the vessel volume, including the radial expansion (diameter) and lengthening, the enlargement due to hypertension represented an equivalent aging of 5-, 6- and 2-years for the ascending, arch and descending segments, respectively. Similarly, the unfolding process was mostly evidenced with an increase of the aortic arch width (+4 years), radius of curvature (+8 years) and a reduction of tortuosity (+7 years). Analyzing BP components, whereas diastolic BP was associated with distention and unfolding of the whole vessel, systolic BP mostly affected TA arch and descending portions. Systolic BP dominated the arch widening, attaining 12% for a 10 mm Hg increase. This study shows that non-contrast multislice computed tomography scans, initially designated to assess calcifications, can provide extra-coronary geometric information to reconstruct the TA in three-dimensions.

Table 2. Thoracic aorta geometric measurements: Absolute values for normotensive vs hypertensive patients and a multivariate regression model adjusted for age

Size and shape measures	Normotensive		Hypertensive		Multivariable model adjusted for age				
	n = 200 men Mean ± s.d.	n = 200 men Mean ± s.d.	(%) change	P	$\beta_{AGE} \pm s.e.$ (10 years aging)	$\beta_{HTA} \pm s.e.$ (hypertension)	β_{HTA} (%) change	$\beta_{HTA} \times 10 / \beta_{AGE}$ (aging effect of HTA (years))	R
Ascending aorta									
Mean diameter, cm	3.23 ± 0.33	3.45 ± 0.34	7	<0.001	0.14 ± 0.02 [‡]	0.07 ± 0.02 [‡]	2	+5	0.45 [‡]
Volume, cm ³	51 ± 14	60 ± 16	17	<0.001	6.2 ± 0.9 [‡]	3.1 ± 0.7 [‡]	6	+5	0.45 [‡]
Aortic arch									
Mean diameter, cm	2.81 ± 0.23	2.97 ± 0.23	6	<0.001	0.11 ± 0.01 [‡]	0.05 ± 0.01 [‡]	2	+5	0.51 [‡]
Volume, cm ³	18 ± 6	22 ± 7	22	<0.001	2.0 ± 0.4 [‡]	1.2 ± 0.3 [‡]	7	+6	0.36 [‡]
Descending aorta									
Mean diameter, cm	2.55 ± 0.20	2.68 ± 0.20	5	<0.001	0.11 ± 0.01 [‡]	0.04 ± 0.01 [‡]	2	+4	0.55 [‡]
Volume, cm ³	83 ± 20	96 ± 23	16	<0.001	13.1 ± 1.1 [‡]	3.0 ± 1.0 [‡]	4	+2	0.57 [‡]
Aortic curvilinear portion (0°–180°)									
Arch width, cm	7.67 ± 0.98	8.38 ± 1.02	9	<0.001	0.56 ± 0.05 [‡]	0.21 ± 0.05 [‡]	3	+4	0.56 [‡]
Radius of curvature, cm	3.17 ± 0.44	3.43 ± 0.45	8	<0.001	0.13 ± 0.03 [‡]	0.10 ± 0.02 [‡]	3	+8	0.37 [‡]
Tortuosity	0.85 ± 0.18	0.80 ± 0.17	–6	<0.01	–0.03 ± 0.01*	0.02 ± 0.01*	2	+7	0.17 [†]
Arch height, cm	4.67 ± 0.65	4.86 ± 0.70	4	<0.01	0.23 ± 0.04	NS	—	—	0.31 [‡]
Tapering, cm/10 cm length	–0.48 ± 0.15	–0.51 ± 0.19	6	0.06	NS	0.02 ± 0.01*	–4	—	NS
Center to 45° distance, cm	4.21 ± 0.50	4.47 ± 0.50	6	<0.001	0.26 ± 0.03 [‡]	0.06 ± 0.02 [†]	1	+2	0.49 [‡]
Center to 135° distance, cm	4.39 ± 0.62	4.76 ± 0.66	8	<0.001	0.32 ± 0.04 [‡]	0.10 ± 0.03 [‡]	2	+3	0.49 [‡]
Area under the arch curve, cm ²	28.3 ± 6.3	32.2 ± 7.1	14	<0.001	3.60 ± 0.36 [‡]	1.00 ± 0.31 [†]	4	+3	0.51 [‡]

Percentage changes are calculated with respect to mean normotensive values adopted as a reference. [‡]P < 0.001, [†]P < 0.01. *P < 0.05.

Segmentation algorithm

At first, we have to emphasize that the automated tool was able to isolate the TA and to estimate the three-dimensional geometry with a high reproducibility rate and accuracy in less than 1 min. True orthogonal aortic sections are assessed in ≈ 180 sites all along the TA centerline, overcoming the traditional limitation of measuring only ascending and descending diameters (Figure 2). Furthermore, the coordinates of the centerline points are determined during this process, allowing to calculate volume and deformation descriptors that are significantly involved in the aortic structural alterations.^{9,10}

Hypertension role on TA size and shape

Associations of age with TA size are consistent with those previously discussed with TA diameter^{3,7,8,14} and justify to assess the potential role of hypertension in terms of aging. Hypertension was found a strong independent determinant factor for size increase in the three TA segments, confirming its major influence on TA enlargement.^{9,14,18} In a multivariate model adjusted for age, the impact of hypertension on TA geometry was evaluated calculating an equivalent factor in years of aging (Table 2). Overall, the presence of hypertension increased 2% TA diameters and 4–7% TA volumes, equivalent to an aging of ≈ 5 -years. The less affected segment was the descending portion. In terms of curvilinear deformation, hypertension produced an equivalent aging of 8-years for the radius of curvature and 7-years for tortuosity. The rest of the parameters, except the arch height and tapering, accounted for an aging of 3–4-years. These results

show that the TA unfolding process that progresses with aging is accelerated in the presence of hypertension.

We also analyzed the relation between TA geometry and BP variables in a multivariate model adjusted for age and hypertensive treatment (Table 3). We observed that TA size evenly increased along its length with diastolic BP. Also, diastolic BP was positively associated with the radius of curvature, the aortic arch width, the 45° and 135° vectors and the AUC. Probably, the relative constant diastolic BP value along the arterial tree reflects the minimum tension that is permanently stimulating the vessel wall and might have a key role in aortic geometric evolution. Systolic BP values were stronger associated with changes in TA size, mostly in the arch and descending portions. Regarding the vessel shape, the aortic arch width and radius of curvature were also sensitive to systolic BP. The role of systolic BP on the proximal aortic size is controversial. Certain studies have reported negative^{1,14,15,18} while others have showed positive associations.^{19,20} The classic notion that associates aging with systolic BP increase is based on a wave propagation argument and suggests a sequence of elastic fragmentation, aortic stretching, wall stiffening and pressure wave acceleration that amplifies systolic BP.^{2,21} On the contrary, several studies reported aortic enlargement with increasing diastolic BP and reduction with increasing systolic BP.^{14,15,22,23} These associations were confirmed in a recent report that studied a community-based data of more than 4500 individuals followed for 16 years.¹ In this longitudinal study, a dynamic remodeling that expands the aortic size is proposed as a compensatory mechanism to limit the systolic BP increase. In fact, a vessel expansion would induce a striking drop of the characteristic impedance to weaken pulsatile components.²⁴

Table 3. Associations of geometric measurements with BP components after adjustment for age and hypertension treatment

Size and shape measures (units per 10 mm Hg increase in BP)	Diastolic BP			Systolic BP		
	$\beta \pm s.e.$	(%) change	R	$\beta \pm s.e.$	(%) change	R
<i>Ascending aorta</i>						
Mean diameter, cm	0.08 ± 0.02 [‡]	2	0.48 [‡]	0.03 ± 0.01*	1	0.44 [‡]
Volume, cm ³	2.9 ± 0.8 [‡]	6	0.47 [‡]	NS	—	0.44 [‡]
<i>Aortic arch</i>						
Mean diameter, cm	0.06 ± 0.01 [‡]	2	0.56 [‡]	0.03 ± 0.01 [†]	1	0.57 [‡]
Volume, cm ³	1.5 ± 0.3 [‡]	8	0.40 [‡]	0.7 ± 0.2 [†]	4	0.37 [‡]
<i>Descending aorta</i>						
Mean diameter, cm	0.05 ± 0.01 [‡]	2	0.59 [‡]	0.03 ± 0.01 [‡]	1	0.57 [‡]
Volume, cm ³	5.1 ± 1.0 [‡]	6	0.61 [‡]	2.5 ± 0.7 [‡]	3	0.59 [‡]
<i>Aortic curvilinear portion (0°–180°)</i>						
Arch width, cm	0.21 ± 0.05 [‡]	3	0.57 [‡]	0.91 ± 0.04 [‡]	12	0.56 [‡]
Radius of curvature, cm	0.08 ± 0.02 [†]	3	0.39 [‡]	0.05 ± 0.01 [†]	2	0.37 [‡]
Tortuosity,	NS	—	0.17 [†]	− 0.01 ± 0.00*	− 1	0.20 [†]
Arch height, cm	NS	—	0.32 [‡]	NS	—	0.32 [‡]
Tapering, cm/10 cm length	NS	—	NS	NS	—	NS
Center to 45° distance, cm	0.09 ± 0.03 [‡]	2	0.51 [‡]	NS	—	0.50 [‡]
Center to 135° distance, cm	0.13 ± 0.03 [‡]	3	0.51 [‡]	0.05 ± 0.02*	1	0.49 [‡]
Area under the arch curve, cm ²	1.03 ± 0.34 [‡]	4	0.52 [‡]	NS	—	0.51 [‡]

Abbreviations: BP, blood pressure; NS, non significant. Data are mean ± s.e. values per 10 mm Hg increase in BP and % change with respect to normotensive population mean values in Table 2. [‡] $P < 0.001$, [†] $P < 0.01$. * $P < 0.05$.

Therefore, an aortic root dilatation could be part of an adaptation mechanism to reduce the characteristic impedance and the systolic BP. In addition, it was reported that the increase in systolic BP within hypertensive subjects could be attributed to aortic stiffening and a mitigated aortic size expansion rather than to wave propagation causes.¹⁸ It is to note that the inverse relation between systolic BP and aortic size can be also predicted from elastic modulus or characteristic impedance estimations.^{15,24} In our opinion, there is a propensity to directly associate systolic BP with aortic size, which is contaminated by the aging effect. In the present study, we find that TA size has a strong dependence on diastolic BP in all its segments but we observed that systolic BP was mostly associated to a descending TA expansion. All these effects could be thought in the mentioned context of a remodeling process that expands the proximal TA portion, limiting the systolic BP. Further studies are needed to confirm these observations.

Study limitations

The measurement of BP in the brachial artery, and not centrally, may induce some distortions that need to be discussed. In particular, we found that brachial systolic BP was not strongly associated to the size of the ascending TA (Table 3). We consider that TA size associations with central pressure components would remain unaffected with respect to brachial measurements, as shown in other studies.^{9,24} Chen *et al.* proposed a general transfer function to estimate central aortic pressure waveform from a radial tonometry.²⁵ Using their regression models to convert brachial to central systolic and diastolic values, we verified that results in Table 3 remained unchanged. Furthermore, assuming an amplification effect, central systolic BP values would result lower, reducing even more the weak association we found with ascending TA size. As tonometry was not available in our study, further measurements are required to elucidate the specific role of systolic BP. Additionally, and due to the absence of contrast

imaging, TA cross-sectional measures represent the sum of the vessel wall and the lumen, impeding to discriminate whether an increase in aortic volume is due to true luminal enlargement or to compensatory remodeling in response to wall plaque. We are also aware that the exact definition of the TA segments in our work may not match with other reports and then comparisons should be made with caution for the segments length and volume.^{9,10} In the TA exploration, primarily intended for CAC measurement, the field of view was extended to cover the aortic arch. The total scan length in our protocol was 10–15% higher with respect to routinely CAC scans. Such extended scan length has an additional radiation dose cost for the patient but offers the benefit of extra-coronary measures like the ones proposed in our study or even further complete TA calcification assessments that contain the aortic arch. Aortic valve disease is known to be associated with an aortopathy but it was not systematically evaluated in our study except by echocardiography in those patients with heart murmur at auscultation or those with electrocardiography abnormalities, which represented a very small proportion in our sample. Screening patients with aortic valve disease such as bicuspid valve or aortic stenosis may be performed in future studies. Lastly, the cross-sectional design of our study does not allow assessing the time-dependent and causal relationships between parameters.

In conclusion, in this work we showed that hypertension accelerates the aortic enlargement and collaborates with the aortic arch widening process. Globally, the presence of hypertension was equivalent to a 5-years-old aging. Measures were assessed using an original non-invasive method capable of measuring accurately and rapidly TA geometry from non-contrast CT scans. Whereas diastolic BP was associated to TA enlargement in its three segments, systolic BP was mostly related with changes in the aortic arch and descending portions. Using this new methodology, further studies could be proposed to accurately assess the differential impact of other determinant risk factors on TA size and shape.

What is known about this topic

- Aging and hypertension are determinant risk factors that are involved in changes of the thoracic aorta geometry.
- Non-contrast CT is employed as a noninvasive method to estimate aortic enlargement by measuring two single diameters in the ascending and descending portions.
- Several studies report aortic size progression whereas less is known about aortic regional and three-dimensional shape evolution.

What this study adds

- Hypertension accelerates thoracic aorta enlargement and the aortic arch widening process, independently of aging.
- The presence of hypertension was found to produce an equivalent 5-years-old aging on aortic deformation, mostly evidenced in the ascending and aortic arch portions.
- Diastolic BP was associated to size and shape changes in the entire thoracic aorta whereas systolic BP had an effect mostly on aortic arch and descending portions.

CONFLICT OF INTEREST

The authors declare no conflict of interest.

ACKNOWLEDGEMENTS

This work was partially supported by post-doctoral scholarship cooperation program between France and Argentina 'Bernardo Houssay'. We thank Mrs Latifa Boudali for her invaluable assistance in database management.

REFERENCES

- Lam CS, Xanthakis V, Sullivan LM, Lieb W, Aragam J, Redfield MM *et al*. Aortic root remodeling over the adult life course: longitudinal data from the Framingham Heart Study. *Circulation* 2010; **122**: 884–890.
- O'Rourke M, Farnsworth A, O'Rourke J. Aortic dimensions and stiffness in normal adults. *JACC Cardiovasc Imaging* 2008; **1**: 749–751.
- Wolak A, Gransar H, Thomson LEJ, Friedman JD, Hachamovitch R, Gutstein A *et al*. Aortic size assessment by noncontrast cardiac computed tomography: normal limits by age, gender, and body surface area. *JACC: Cardiovascular Imaging* 2008; **1**: 200–209.
- Elefteriades JA, Farkas EA. Thoracic aortic aneurysm clinically pertinent controversies and uncertainties. *J Am Coll Cardiol* 2010; **55**: 841–857.
- Hinchliffe RJ, Krasznai A, Schultzekool L, Blankensteijn JD, Falkenberg M, Lonn L *et al*. Observations on the failure of stent-grafts in the aortic arch. *Eur J Vasc Endovasc Surg* 2007; **34**: 451–456.
- Melissano G, Civolini E, Bertoglio L, Calliari F, Setacci F, Calori G *et al*. Results of endografting of the aortic arch in different landing zones. *Eur J Vasc Endovasc Surg* 2007; **33**: 561–566.
- Mao SS, Ahmadi N, Shah B, Beckmann D, Chen A, Ngo L *et al*. Normal thoracic aorta diameter on cardiac computed tomography in healthy asymptomatic adults: impact of age and gender. *Acad Radiol* 2008; **15**: 827–834.
- Chironi G, Orobinskaia L, Megnien JL, Sirieix ME, Clement-Guinaudeau S, Bensalah M *et al*. Early thoracic aorta enlargement in asymptomatic individuals at risk for cardiovascular disease: determinant factors and clinical implication. *J Hypertens* 2010; **28**: 2134–2138.
- Redheuil A, Yu WC, Mousseaux E, Harouni AA, Kachenoura N, Wu CO *et al*. Age-related changes in aortic arch geometry: relationship with proximal aortic function and left ventricular mass and remodeling. *J Am Coll Cardiol* 2011; **58**: 1262–1270.
- Sugawara J, Hayashi K, Yokoi T, Tanaka H. Age-associated elongation of the ascending aorta in adults. *J Am Coll Cardiol Img* 2008; **1**: 739–748.
- Craiem D, Chironi G, Redheuil A, Casciaro M, Mousseaux E, Simon A *et al*. Aging impact on thoracic aorta 3D morphometry in intermediate-risk subjects: looking beyond coronary arteries with non-contrast cardiac CT. *Ann Biomed Eng* 2012; **40**: 1028–1038.
- Greenland P, Alpert JS, Beller GA, Benjamin EJ, Budoff MJ, Fayad ZA *et al*. 2010ACCF/AHA guideline for assessment of cardiovascular risk in asymptomatic adults: a report of the American College of Cardiology Foundation/American Heart Association Task Force on Practice Guidelines. *J Am Coll Cardiol* 2010 **56**: e50–103.
- Chironi G, Simon A, Megnien JL, Sirieix ME, Mousseaux E, Pessana F *et al*. Impact of coronary artery calcium on cardiovascular risk categorization and lipid-lowering drug eligibility in asymptomatic hypercholesterolemic men. *Int J Cardiol* 2011; **151**: 200–204.
- Agmon Y, Khandheria BK, Meissner I, Schwartz GL, Sicks JD, Fought AJ *et al*. Is aortic dilatation an atherosclerosis-related process? Clinical, laboratory, and transesophageal echocardiographic correlates of thoracic aortic dimensions in the population with implications for thoracic aortic aneurysm formation. *J Am Coll Cardiol* 2003; **42**: 1076–1083.
- Vasan RS, Larson MG, Levy D. Determinants of echocardiographic aortic root size. The Framingham Heart Study. *Circulation* 1995; **91**: 734–740.
- Zhao F, Zhang H, Wahle A, Thomas MT, Stolpen AH, Scholz TD *et al*. Congenital aortic disease: 4D magnetic resonance segmentation and quantitative analysis. *Med Image Anal* 2009; **13**: 483–493.
- Wood NB, Zhao SZ, Zambanini A, Jackson M, Gedroyc W, Thom SA *et al*. Curvature and tortuosity of the superficial femoral artery: a possible risk factor for peripheral arterial disease. *J Appl Physiol* 2006; **101**: 1412–1418.
- Mitchell GF, Conlin PR, Dunlap ME, Lacourciere Y, Arnold JM, Ogilvie RI *et al*. Aortic diameter, wall stiffness, and wave reflection in systolic hypertension. *Hypertension* 2008; **51**: 105–111.
- Ingelsson E, Pencina MJ, Levy D, Aragam J, Mitchell GF, Benjamin EJ *et al*. Aortic root diameter and longitudinal blood pressure tracking. *Hypertension* 2008; **52**: 473–477.
- Jondeau G, Boutouyrie P, Lacombe P, Laloux B, Dubourg O, Bourdarias JP *et al*. Central pulse pressure is a major determinant of ascending aorta dilation in Marfan syndrome. *Circulation* 1999; **99**: 2677–2681.
- O'Rourke MF, Nichols WW. Aortic diameter, aortic stiffness, and wave reflection increase with age and isolated systolic hypertension. *Hypertension* 2005; **45**: 652–658.
- Bella JN, Wachtell K, Boman K, Palmieri V, Papademetriou V, Gerds E *et al*. Relation of left ventricular geometry and function to aortic root dilatation in patients with systemic hypertension and left ventricular hypertrophy (the LIFE study). *Am J Cardiol* 2002; **89**: 337–341.
- Cuspidi C, Meani S, Fusi V, Valerio C, Sala C, Zanchetti A. Prevalence and correlates of aortic root dilatation in patients with essential hypertension: relationship with cardiac and extracardiac target organ damage. *J Hypertens* 2006; **24**: 573–580.
- Mitchell GF, Lacourciere Y, Ouellet JP, Izzo Jr. JL, Neutel J, Kerwin LJ *et al*. Determinants of elevated pulse pressure in middle-aged and older subjects with uncomplicated systolic hypertension: the role of proximal aortic diameter and the aortic pressure-flow relationship. *Circulation* 2003; **108**: 1592–1598.
- Chen CH, Nevo E, Fetis B, Pak PH, Yin FC, Maughan WL *et al*. Estimation of central aortic pressure waveform by mathematical transformation of radial tonometry pressure. Validation of generalized transfer function. *Circulation* 1997; **95**: 1827–1836.